COVER SHEET

Thermal decomposition and X-ray diffraction of sulphate efflorescent minerals from El Jaroso Ravine, Sierra Almagrera, Spain

Ray L. Frost [a•], Daria Wain [a], Wayde N. Martens [a], Ashley C. Locke [a] Jesus Martinez-Frias [a,b] and Fernando Rull [a,b]

[a] Inorganic Materials Research Program, School of Physical and Chemical Sciences, Queensland University of Technology, GPO Box 2434, Brisbane Queensland 4001, Australia.

[b] Cristalografia y Mineralogia. Unidad Asociada al Centro de Astrobiologia INTA-CSIC. Universidad de Valladolid. 47006, Valladolid, Spain.

Abstract

Two evaporite minerals fro the El Jaroso Ravine, Spain have been analysed by thermogravimetry coupled with an evolved gas mass spectrometer. X-ray diffraction results proved the evaporite minerals were a mixture of sulphates including the minerals magnesiocopiapite, coquimbite and possibly alunogen. Thermal decomposition of the unoxidised samples showed steps at 52, 99, 143°C confirmed by mass spectrometric results and attributed to adsorbed water, interstitial water and chemically bonded water. This evaporite mineral rock showed two higher temperature decomposition steps at 555 and 599°C with mass losses of 19.6 and 7.8%. Slightly different temperatures for the thermal decomposition of the oxadada sample were observed at 52, 64.5 and 100°C. Two higher temperature mass loss steps at 560.5 and 651°C were observed for the oxidised sample. By comparison of the thermal analysis patterns of halotrichite and jarosite it can be shown that the El Jaroso samples are mineral sulphates and not halotrichite or jarosite.

Keywords: evaporite, jarosite, sulphate, dehydration, dehydroxylation, halotrichite, TG-MS, high-resolution thermogravimetric analysis

Introduction

The jarosite mineral group has been extensively studied [1]. Jarosite was first discovered on Earth in 1852 in ravines in the mountainous coast of south eastern Spain. Since this time, the jarosite minerals were mined extensively for silver jarosite. This has resulted in the formation of evaporite minerals as is found in the El Jaroso Ravine, Sierra Almagrera, Spain. The importance of jarosite formation and its decomposition depends upon its presence in mine tailings, soils, sediments and evaporite deposits [2]. These types of deposits are formed in acid soils where the pH is less than 3.0 pH units [3]. Such acidification results from the oxidation of pyrite which may be from bacterial action or through air-oxidation. The Mars mission rover known as opportunity has been used to discover the presence of jarosite on Mars, thus providing evidence for the existence or pre-existence of water on Mars. Interest in evaporite minerals and

• Author to whom correspondence should be addressed (r.frost@qut.edu.au)

their thermal stability rests with the possible identification of these minerals and related dehydrated paragenetically related mineral on planets and on Mars. The existence of these minerals on planets would give a positive indication of the existence or at least pre-existence of water on Mars. Further such minerals are formed through crystallization from solutions.

The thermal decomposition of evaporite mineral mixtures such as those found in the El Jaroso Ravine, Sierra Almagrera, Spain has not been studied [4-8]. There have been many studies on related minerals such as the Fe(II) and Fe(III) sulphate minerals [9-14]. It has been stated that the thermal decomposition of jarosite begins at 400 °C with the loss of water [1]. The process is apparently kinetically driven. Water loss can occur at low temperatures over extended periods of time [1]. It is probable that in nature low temperature environments would result in the decomposition of jarosite. The products of the decomposition depend upon the jarosite be it K, Na or Pb etc but normally goethite and hematite are formed together with soluble sulphates [15]. Recently thermogravimetric analysis has been applied to some complex mineral systems and it is considered that TG-MS analyses may also be applicable to the jarosite minerals [16-21]. Raman spectroscopy has proven very useful for the study of these types of minerals [22-24]. Indeed Raman spectroscopy has proven most useful for the study of diagenetically related minerals as often occurs with carbonate minerals [25-29]. Some previous studies have been undertaken by the authors using Raman spectroscopy to study complex secondary minerals formed by crystallization from concentrated sulphate solutions [30]. In this work we report the XRD and thermogravimetric analysis of two evaporite mineral mixtures from the El Jaroso Ravine, Spain.

Experimental

Minerals

The evaporite minerals were collected by two of the authors (FR and JM). The minerals originated from El Jaroso Ravine, Sierra Almagrera, Spain [see http://tierra.rediris.es/jarosite/]. The two mineral mixture containing samples are labelled as eflorescencia and eflorescencia oxadada. The evaporite minerals were analysed by X-ray diffraction for phase purity and by electron probe using energy dispersive techniques for quantitative chemical composition. The Na-jarosite was found to contain some K but at low concentration levels.

X-Ray diffraction

X-ray diffraction (XRD) patterns were recorded using CuKα radiation (n = 1.5418Å) on a Philips PANalytical X' Pert PRO diffractometer operating at 40 kV and 40 mA with 0.125° divergence slit, 0.25° anti-scatter slit, between 3 and 15° (2θ) at a step size of 0.0167°. For low angle XRD, patterns were recorded between 1 and 5° (2θ) at a step size of 0.0167° with variable divergence slit and 0.5° anti-scatter slit.

Thermal Analysis

Thermal decomposition of the evaporate rocks were carried out in a TA® Instruments incorporated high-resolution thermogravimetric analyzer (series Q500) in a flowing nitrogen atmosphere (80 cm^3/min). 34.4 mg of sample underwent thermal analysis, with a heating rate of 5°C/min, resolution of 6°C, to 1000°C. With the quasi-isothermal, quasi-isobaric heating program of the instrument the furnace temperature was regulated precisely to provide a uniform rate of decomposition in the main decomposition stage. The TGA instrument was coupled to a Balzers (Pfeiffer) mass spectrometer for gas analysis. Only water vapour, carbon dioxide and oxygen were analyzed.

Results and discussion

X-ray diffraction

The XRD patterns of the evaporite samples eflorescencia, halotrichite and Na jarosite are shown in Figures 1a, 1b, 1c respectively. XRD patterns are taken from a powdered sample and so will be representative of a mixture. Another difficulty is that the sample does contain amorphous and/or non diffracting materials. Therefore powder XRD may not give the total story of the efflorescent minerals. Hence this is the fundamental reason why techniques such as thermal analysis are used to analyse these types of mineral mixtures. The XRD pattern of the eflorescencia matches the sum of the XRD patterns of magnesiocopiapite ($MgFe_4(SO_4)_6.20H_2O$), coquimbite ($Fe_2(SO_4)_3.9H_2O$) and probably alunogen ($Al_2(SO_4)_3.17H_2O$). The XRD patterns show the eflorescencia is a complex mixture of sulphates. Figure 1a shows the XRD patterns of the oxadada rock. The analysis is similar to that for the eflorescencia sample. The difference between the two XRD patterns rests with the change in the ratio of magnesiocopiapite, coquimbite and possibly alunogen. For comparison, Figure 1b shows the XRD patterns of two halotrichites from Spain and California together with the reference patterns of pickingerite and apjohnite. The halotrichite from Spain is a mixture of pickingerite, apjohnite and heinrichite. The Na jarosite from Spain is predominantly Na jarosite together with some impurities. The XRD patterns of the Na jarosite do show resemblance to the patterns of the evaporite minerals. Na jarosite may be present in the evaporite minerals. It is difficult to be precise.

Thermogravimetric and Mass spectrometric analysis of evaporite minerals

The TG and DTG patterns of the efflorescencia sample are shown in Figure 2. The ion current curves are reported in Figures 3a (M/Z=18 and 32) and 3b (M/Z= 38, 48, 64, 44). The TG and DTG of the oxidised sample [efflorescencia oxadada] are shown in Figure 4. For comparison the TG and DTG curves for a Na-jarosite are shown in Figure 6 and the ion current curves for Na-jarosite in Figures 7a and 7b.

Thermal decomposition steps in the low temperature region are observed for the eflorescencia sample at 52, 99, 143°C (Figure 2). The mass losses are 6.3, 2.2 and 9.6%. Ion current curves for M/Z =18 shows a maxima at 119°C and for M/Z=32 at 52, 96 and 142 °C. These peaks are attributed to the loss of water. The decomposition steps for the efflorescent sample may be given as follows:

Step 1 Temperature 53 °C

$MgFe_4(SO_4)_6.20H_2O \rightarrow MgFe_4(SO_4)_6.\ xH_2O + (20\text{-}x)H_2O$

$Fe_2(SO_4)_3.9H_2O \rightarrow Fe_2(SO_4)_3.yH_2O + (9\text{-}y)H_2O$

This step represents the loss of water or partial loss of water from the hydrated minerals. The chemical reactions are exemplary only and do not show alunogen which may not be present or where some amorphous mineral of a similar formula is present.

Step 2 Temperature 99 and 143°C

$MgFe_4(SO_4)_6.\ xH_2O \rightarrow MgFe_4(SO_4)_6.\ + xH_2O$

$Fe_2(SO_4)_3.yH_2O \rightarrow\ Fe_2(SO_4)_3 + yH_2O$

This step represents the complete loss of water.

Step 3 Temperature 555 and 599°C

$MgFe_4(SO_4)_6\ \rightarrow\ MgO + 2Fe_2O_3 + 4SO_3$

$Fe_2(SO_4)_3\ \rightarrow\ Fe_2O_3 + 4SO_3$

These thermal decompositions represent the loss of sulphate as SO_3.
It is likely that a second step occurs as follows

$SO_3 \rightarrow SO_2 + 1/2O_2$

There is a mass loss of 19.6% at 555°C and 7.8% at 599°C

Step 4 Temperature 743 °C

$Fe_2O_3 \rightarrow 2FeO + 1/2O_2$

At this temperature the hematite loses oxygen.

The next decomposition step is observed at around 270°C. A corresponding ion current peak at 267°C for M/Z=32 is observed. The XRD patterns show the presence of magnesiocopiapite ($MgFe_4(SO_4)_6.20H_2O$), coquimbite ($Fe_2(SO_4)_3.9H_2O$) and possibly alunogen ($Al_2(SO_4)_3.17H_2O$) and thus the loss of significant amounts of water is to be expected. Two major mass losses at 555 and 599°C are observed with mass losses of 19.6 and 7.8%. These thermal decomposition steps are attributed to the decomposition of sulphate. The ion current curves for m/Z=48 (SO) and 64 (SO_2) show a complex pattern with maxima at 547, 602, 637, 659 and 741°C. These ion current maxima are attributed to the loss of sulphate from magnesiocopiapite, coquimbite and possible alunogen or some other sulphate of aluminium.

The TG and DTG patterns of the oxadada sample are shown in Figure 4. The thermal decomposition steps and chemical reactions are similar to those above. Three mass loss steps at 52, 64.5 and 100°C are attributed to the loss of adsorbed water and water of hydration. Minor mass losses are observed at 176, 260 and 358°C. The ion current curves for m/Z = 17 and 18 (Figure 5a) show maxima at 51.8, 64 and 100°C indicating the loss of water from the oxadada sample. Another mass loss at 358°C is observed which the ion current curves may be ascribed to the loss of water. Such water molecules must be strongly bonded in the minerals. Two thermal decomposition

steps at 560.5 and 651°C with mass losses of 28.4 and 7.6% are observed with a higher temperature mass loss of 2.9% at 736°C. The ion current curves indicate show some maxima for m/Z at 569, 650 and 730°C. These thermal decomposition steps are attributed to the decomposition of sulphate.

Comparison with the thermal analysis of jarosite and halotrichite

A comparison may be made with the thermal decomposition of sodium jarosite from a similar origin as the eflorescencia samples. The reason for this is that the mineral mixture may not be sufficiently crystalline to give an XRD pattern. Na-jarosite is of a theoretical formula $Na_2(Fe^{3+})_6(SO_4)_4(OH)_{12}$. Electron probe analysis showed that the Na-jarosite contained some 17 % K. Thus the formula of the Na-jarosite would be better written as $(K_{.17}Na_{.83})_2(Fe^{3+})_6(SO_4)_4(OH)_{12}$. The thermogravimetric analysis of natural Na-jarosite is shown in Figure 6. Thermal decomposition steps are observed at (a) 50 and 91°C (b) 214°C (c) 375 °C and (c) 541°C. The ion current curves (Figures 7a and b) for Na-jarosite shows that water vapour is the evolved gas at the first four temperatures and SO_2 is lost at the higher temperatures. There is a 2.7% mass loss due to water loss at 214 °C. This water may be described as "excess water" [31, 32]. It is possible that this water results from the deprotonation of the Na-jarosite. Jarosites have a hydroxyl surface which is capable of adsorbing protons creating a hydrogen-jarosite. Thus the Na-jarosite is a sodium protonated jarosites and the formula may be written as $(H_xK_{.17-x/2}Na_{.83-x/2})_2(Fe^{3+})_6(SO_4)_4(OH)_{12}$. The theoretical mass loss of Na-jarosite based upon the formula $Na_2(Fe^{3+})_6(SO_4)_4(OH)_{12}$ is 11.13 %. If the initial 4 % mass loss is neglected the mass loss at 316 and 352 °C is 10 %. This value is close to the theoretical value. The reaction may be summarised as follows: $Na_2(Fe^{3+})_6(SO_4)_4(OH)_{12} \rightarrow 2NaFe(SO_4)_2 + 2Fe_2O_3 + 6\ H_2O$

The thermogravimetric and differential thermogravimetric analysis of halotrichite are shown in Figure 7. Seven major thermal decomposition steps are observed. Steps 1, 2, 3 and 4 occur at temperatures of 53, 72 and 330 °C. A mass loss of 14.28% is observed at quite low temperatures around or up to 42°C. A further mass loss of 9.20 % occurs at 53°C and 18.91% up to 300°C. A small mass loss of 3.18% is observed at 330°C. Each of these thermal decomposition steps is attributed to dehydration of the halotrichite. The ion current curves for halotrichite of H_2O and OH units show maxima at 72 and 330°C. Using the formula $(Fe_{0.75}^{2+},Mg_{0.25})SO_4.Al_2(SO_4)_3.22H_2O$ the total theoretical mass loss for water is 44.90%. The total experimental mass loss is 45.57% which is in good agreement.

Steps 4, 5, 6, 7 and 8 occur at temperatures of 546, 625, 697 and 738 °C. Four thermal decomposition steps are observed for halotrichite of the above formula at 546, 625, 697 and 738 °C. Each of these steps is assigned to the decomposition of sulphate anions, the formation of the metal oxides and the evolution of SO_2 and O_2. The mass losses at these temperatures are 1.69, 19.03, 7.72 and 7.21% making a total of mass loss of 35.65%. The theoretical mass loss calculated using the above formula is 36.29%. The measured mass loss is in agreement with the theoretical mass loss. This agreement confirms the formula of halotrichite. If the formula was different then the numbers would not be in such close agreement. These decomposition steps are confirmed by the ion current curves of the evolved gases SO_2 and O_2 where ion current maxima at 546, 625, 697 and 738 °C are observed.

Conclusions

Thermogravimetric analysis coupled to a mass spectrometer has been used to study selected mineral samples from the El Jaroso Ravine, Spain. Two samples were analysed firstly an unoxidised sample labelled as eflorescencia and secondly an oxidised sample labelled as eflorescencia oxadata. A comparison is made with the thermal decomposition of a sodium jarosite. X-ray diffraction showed the sample was a complex mixture including the sulphates of magnesiocopiapite, coquimbite and possibly alunogen or some sulphate of aluminium. A difficulty of analysing such mineral materials is that the sample contains amorphous and/or non diffracting materials. Therefore powder XRD may not give the complete story of the efflorescent minerals. Hence this is the reason why other techniques such as thermal analysis may be used to analyse these types of mineral mixtures.

Thermal analysis coupled to evolved gas mass spectrometry showed that the TG of the unoxidised samples had thermal decomposition steps at 52, 99, 143°C confirmed by the mass spectrometric results which are attributed to adsorbed water, interstitial water and chemically bonded water. The eflorescencia sample showed two higher temperature decomposition steps at 555 and 599°C with mass losses of 19.6 and 7.8%. Slightly different temperatures of the thermal decomposition of the oxadada sample are observed at 52, 64.5 and 100°C. Two higher temperature mass loss steps at 560.5 and 651°C are observed for the oxidised sample. The latter value is significantly higher than for the unoxidised sample. A comparison of the thermal decomposition of jarosite and halotrichite confirms that the evaporite minerals are not jarosite or halotrichite but are a mixture of sulphates.

Acknowledgments

The financial and infra-structure support of the Queensland University of Technology Inorganic Materials Research Program of the School of Physical and Chemical Sciences is gratefully acknowledged. The Australian Research Council (ARC) is thanked for funding the thermal analysis facility.

References

1. Dutrizac, J. E. and Jambor, J. L., Chapter 8 Jarosites and their application in hydrometallurgy, 405 (2000).
2. Buckby, T., Black, S., Coleman, M. L. and Hodson, M. E., *Mineralogical Magazine* 67, 263 (2003).
3. Williams, P. A., *Oxide Zone Geochemistry*, Ellis Horwood Ltd, Chichester, West Sussex, England, 1990.
4. Nagai, S. and Yamanouchi, N., *Nippon Kagaku Kaishi (1921-47)* 52, 83 (1949).
5. Kulp, J. L. and Adler, H. H., *American Journal of Science* 248, 475 (1950).
6. Cocco, G., *Periodico di Mineralogia* 21, 103 (1952).
7. Tsvetkov, A. I. and Val'yashikhina, E. P., *Doklady Akademii Nauk SSSR* 89, 1079 (1953).
8. Tsvetkov, A. I. and Val'yashikhina, E. P., *Doklady Akademii Nauk SSSR* 93, 343 (1953).
9. Swamy, M. S. R., Prasad, T. P. and Sant, B. R., *Journal of Thermal Analysis* 16, 471 (1979).
10. Swamy, M. S. R., Prasad, T. P. and Sant, B. R., *Journal of Thermal Analysis* 15, 307 (1979).
11. Bhattacharyya, S. and Bhattacharyya, S. N., *Journal of Chemical and Engineering Data* 24, 93 (1979).
12. Swami, M. S. R. and Prasad, T. P., *Journal of Thermal Analysis* 19, 297 (1980).
13. Swamy, M. S. R. and Prasad, T. P., *Journal of Thermal Analysis* 20, 107 (1981).
14. Banerjee, A. C. and Sood, S., *Therm. Anal., Proc. Int. Conf., 7th* 1, 769 (1982).
15. Thomas, P. S., Hirschausen, D., White, R. E., Guerbois, J. P. and Ray, A. S., *Journal of Thermal Analysis and Calorimetry* 72, 769 (2003).
16. Frost, R. L. and Erickson, K. L., *Journal of Thermal Analysis and Calorimetry* 76, 217 (2004).
17. Frost, R. L., Erickson, K. and Weier, M., *Journal of Thermal Analysis and Calorimetry* 77, 851 (2004).
18. Frost, R. L., Weier, M. L. and Erickson, K. L., *Journal of Thermal Analysis and Calorimetry* 76, 1025 (2004).
19. Frost, R. L. and Weier, M. L., *Journal of Thermal Analysis and Calorimetry* 75, 277 (2004).
20. Frost, R. L., Martens, W., Ding, Z. and Kloprogge, J. T., *Journal of Thermal Analysis and Calorimetry* 71, 429 (2003).
21. Frost, R. L., Ding, Z. and Ruan, H. D., *Journal of Thermal Analysis and Calorimetry* 71, 783 (2003).
22. Frost, R. L., Palmer, S. J., Bouzaid, J. M. and Reddy, B. J., *Journal of Raman Spectroscopy* 38, 68 (2007).
23. Frost, R. L., Henry, D. A., Weier, M. L. and Martens, W., *Journal of Raman Spectroscopy* 37, 722 (2006).
24. Frost, R. L., Musumeci, A. W., Kloprogge, J. T., Adebajo, M. O. and Martens, W. N., *Journal of Raman Spectroscopy* 37, 733 (2006).
25. Frost, R. L., Cejka, J., Weier, M. and Martens, W. N., *Journal of Raman Spectroscopy* 37, 879 (2006).

26. Frost, R. L., Weier, M. L., Cejka, J. and Kloprogge, J. T., *Journal of Raman Spectroscopy* 37, 585 (2006).
27. Frost, R. L., Cejka, J., Weier, M. L. and Martens, W., *Journal of Raman Spectroscopy* 37, 538 (2006).
28. Frost, R. L., Weier, M. L., Reddy, B. J. and Cejka, J., *Journal of Raman Spectroscopy* 37, 816 (2006).
29. Frost, R. L., Weier, M. L., Martens, W. N., Kloprogge, J. T. and Kristof, J., *Journal of Raman Spectroscopy* 36, 797 (2005).
30. Frost, R. L., Wills, R.-A., Weier, M. L. and Martens, W., *Journal of Raman Spectroscopy* 36, 435 (2005).
31. Drouet, C. and Navrotsky, A., *Geochimica et Cosmochimica Acta* 67, 2063 (2003).
32. Kubisz, J., *Mineralogia Polonica* 2, 51 (1971).

List of Figures

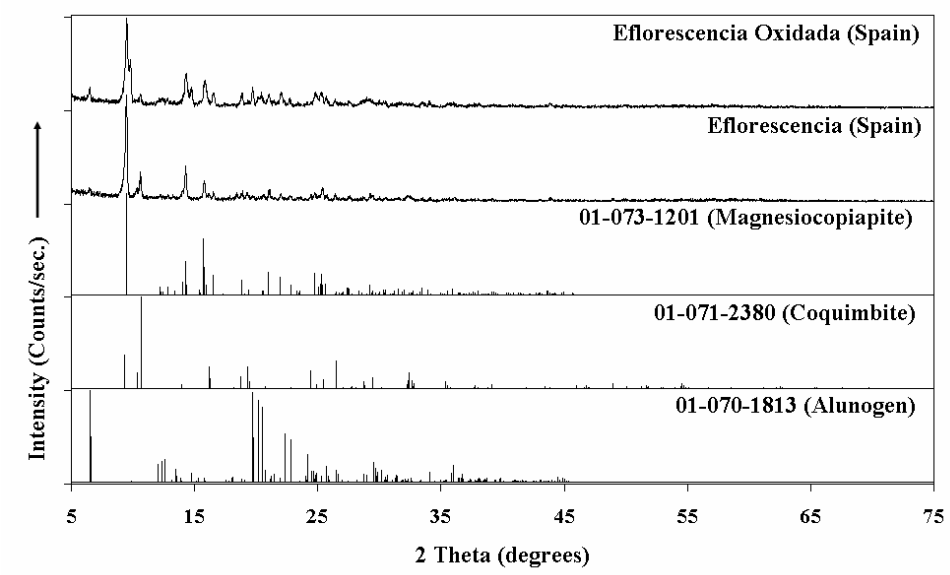
Eflorescencia Oxidada (Spain)
Eflorescencia (Spain)
01-073-1201 (Magnesiocopiapite)
01-071-2380 (Coquimbite)
01-070-1813 (Alunogen)
Intensity (Counts/sec.)
5
15
25
35
45
55
65
75
2 Theta (degrees)

Figure 1a

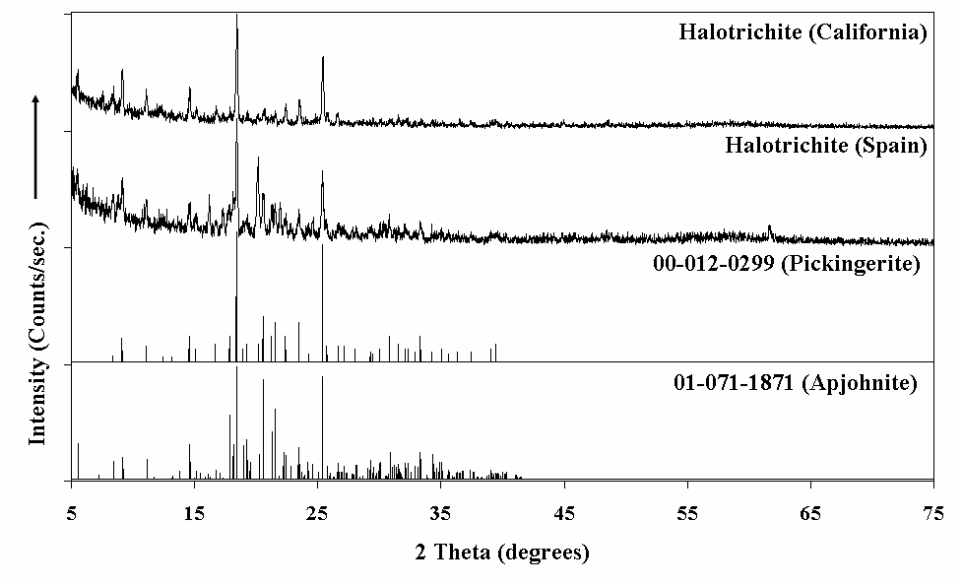
Halotrichite (California)
Halotrichite (Spain)
00-012-0299 (Pickingerite)
01-071-1871 (Apjohnite)
Intensity (Counts/sec.)
5
15
25
35
45
55
65
75
2 Theta (degrees)

Figure 1b

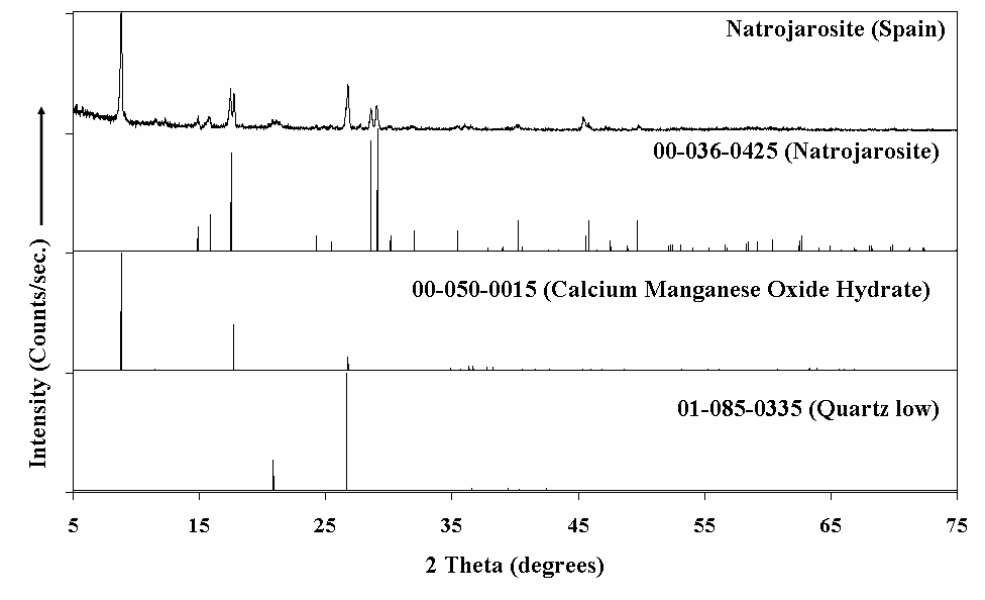
Natrojarosite (Spain)
00-036-0425 (Natrojarosite)
00-050-0015 (Calcium Manganese Oxide Hydrate)
01-085-0335 (Quartz low)
Intensity (Counts/sec.)
5
15
25
35
45
55
65
75
2 Theta (degrees)

Figure 1c

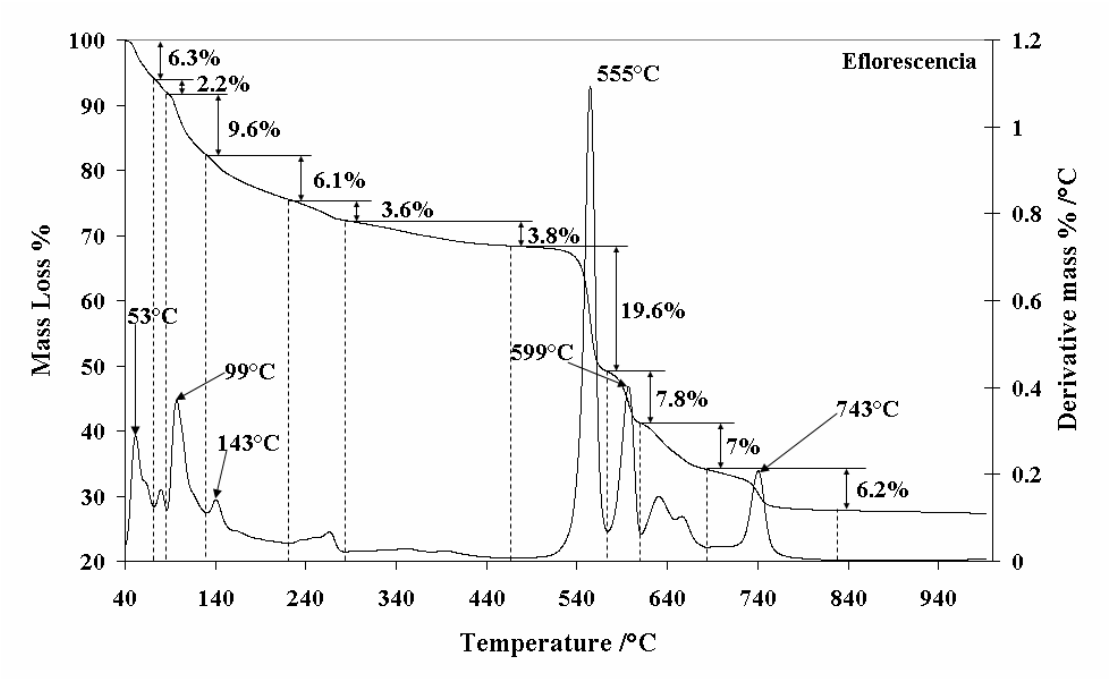
Eflorescencia
Mass Loss %
Derivative mass % /°C
Temperature /°C
6.3%
2.2%
9.6%
6.1%
3.6%
3.8%
19.6%
7.8%
7%
6.2%
53°C
99°C
143°C
555°C
599°C
743°C

Figure 2

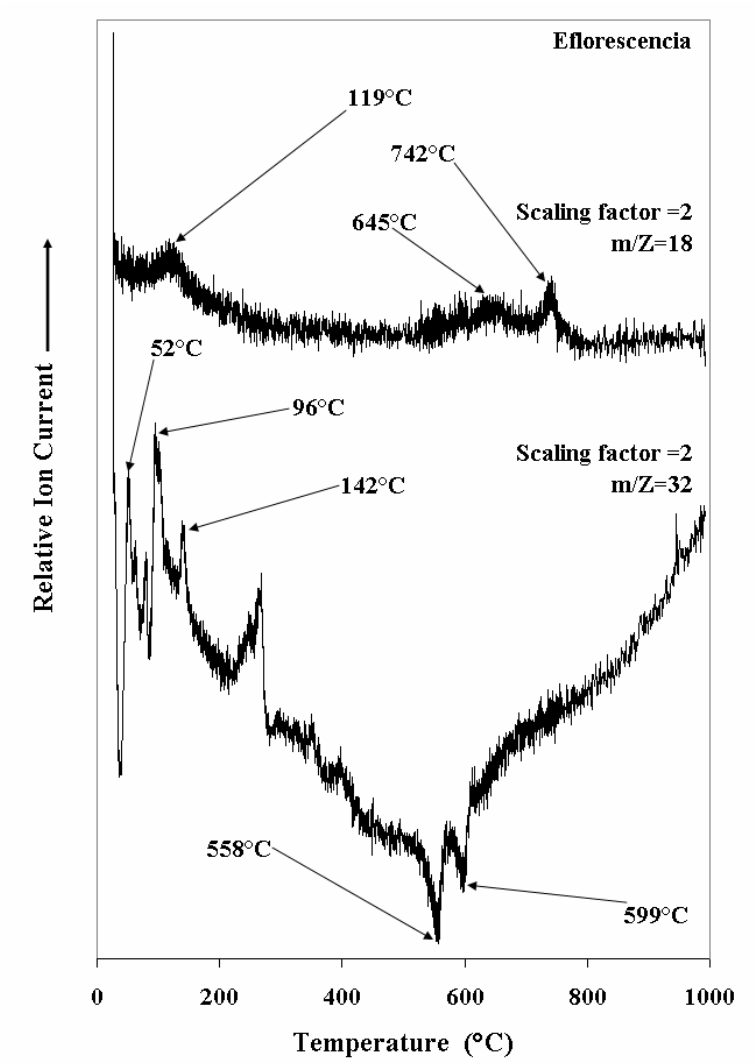
Eflorescencia
119°C
742°C
645°C
Scaling factor =2
m/Z=18
52°C
96°C
Scaling factor =2
m/Z=32
142°C
558°C
599°C
Relative Ion Current
0
200
400
600
800
1000
Temperature (°C)

Figure 3a

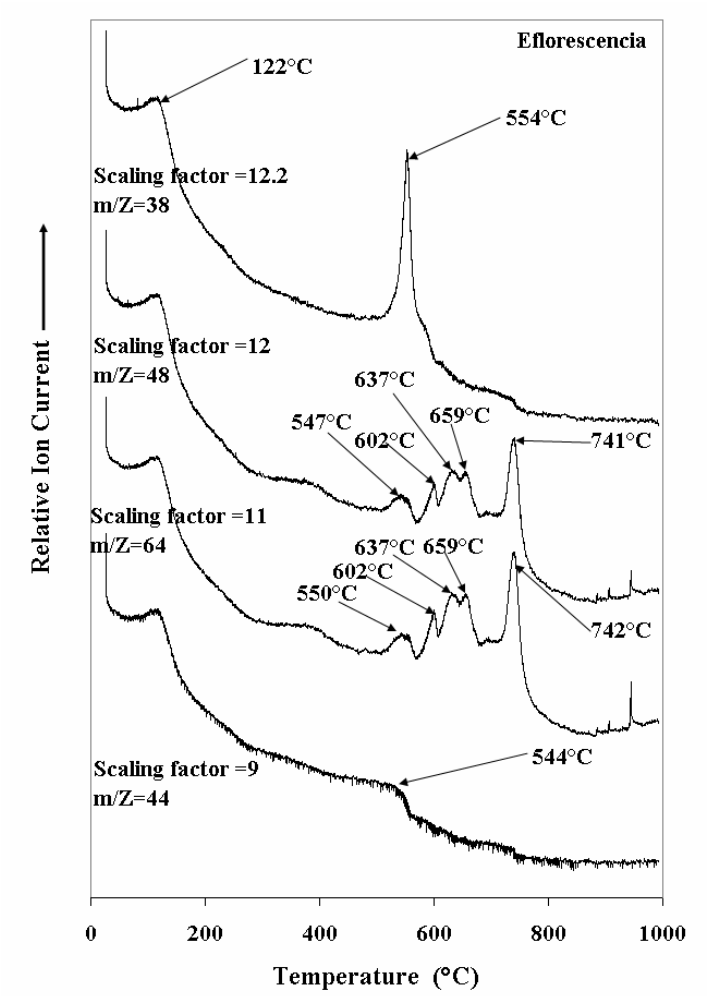
Eflorescencia
122°C
554°C
Scaling factor =12.2
m/Z=38
Scaling factor =12
m/Z=48
637°C
547°C
659°C
602°C
741°C
Scaling factor =11
m/Z=64
637°C
659°C
602°C
550°C
742°C
544°C
Scaling factor =9
m/Z=44
Relative Ion Current
0
200
400
600
800
1000
Temperature (°C)

Figure 3b

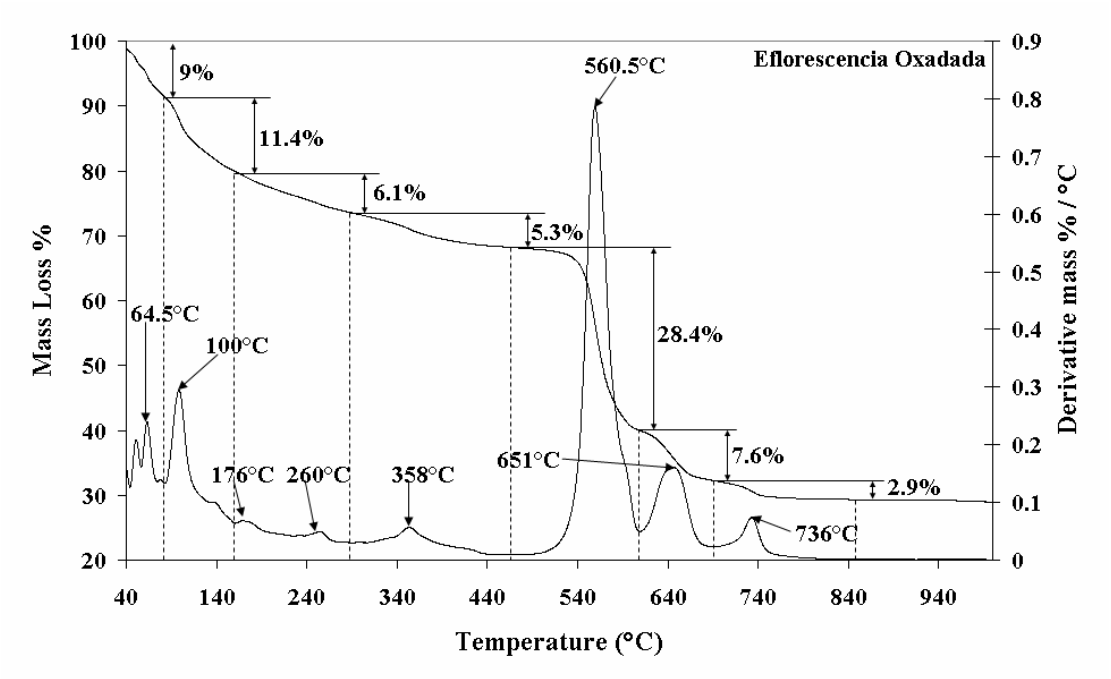
Eflorescencia Oxadada
Mass Loss %
Derivative mass % / °C
Temperature (°C)
9%
11.4%
6.1%
5.3%
28.4%
7.6%
2.9%
64.5°C
100°C
176°C
260°C
358°C
560.5°C
651°C
736°C

Figure 4

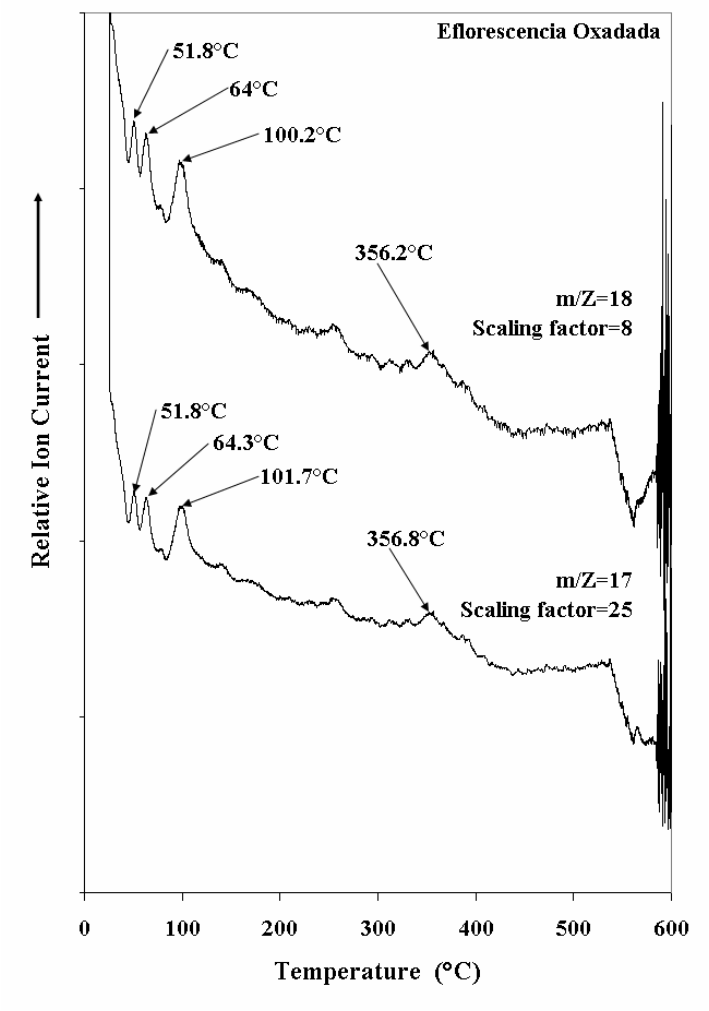
Eflorescencia Oxadada
51.8°C
64°C
100.2°C
356.2°C
m/Z=18
Scaling factor=8
51.8°C
64.3°C
101.7°C
356.8°C
m/Z=17
Scaling factor=25
Relative Ion Current
0
100
200
300
400
500
600
Temperature (°C)

Figure 5a

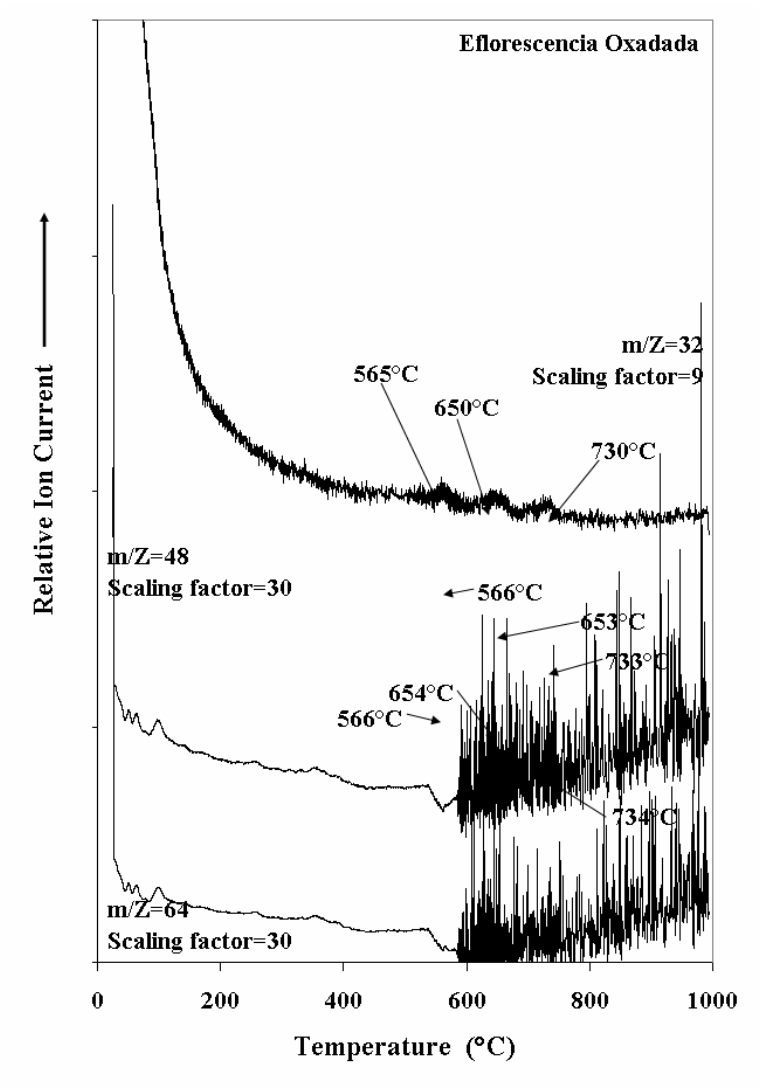
Eflorescencia Oxadada
Relative Ion Current
m/Z=32
Scaling factor=9
565°C
650°C
730°C
m/Z=48
Scaling factor=30
566°C
653°C
733°C
654°C
566°C
734°C
m/Z=64
Scaling factor=30
0
200
400
600
800
1000
Temperature (°C)

Figure 5b

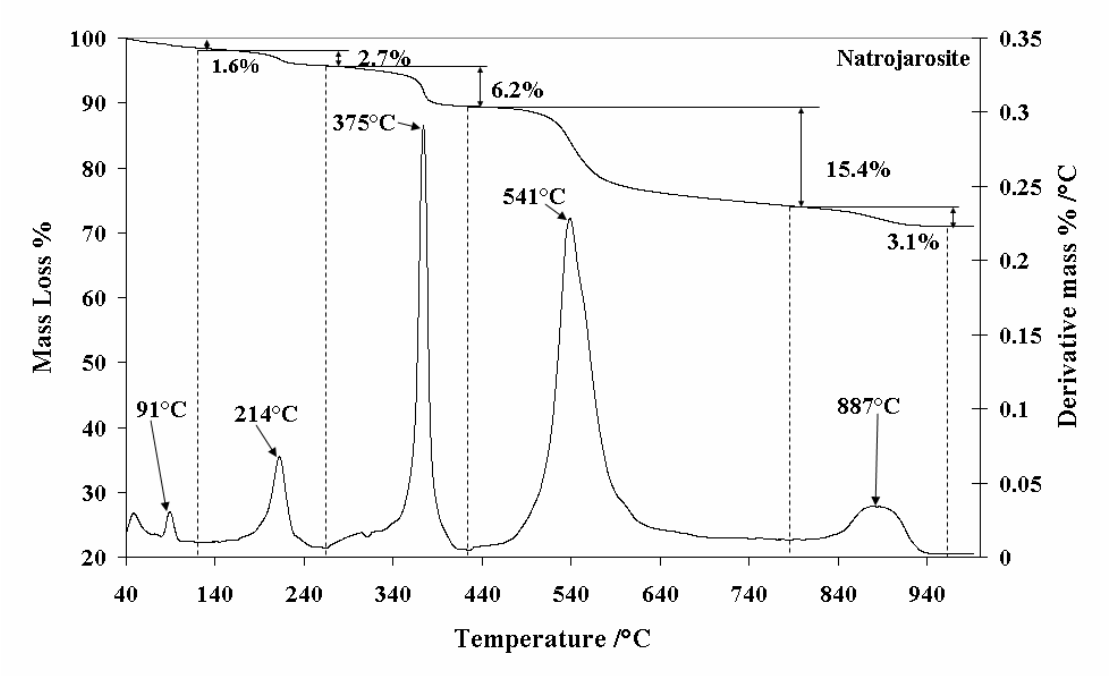
Natrojarosite
1.6%
2.7%
6.2%
15.4%
3.1%
375°C
541°C
91°C
214°C
887°C
Mass Loss %
Derivative mass % /°C
Temperature /°C
100
90
80
70
60
50
40
30
20
0.35
0.3
0.25
0.2
0.15
0.1
0.05
0
40
140
240
340
440
540
640
740
840
940

Figure 6

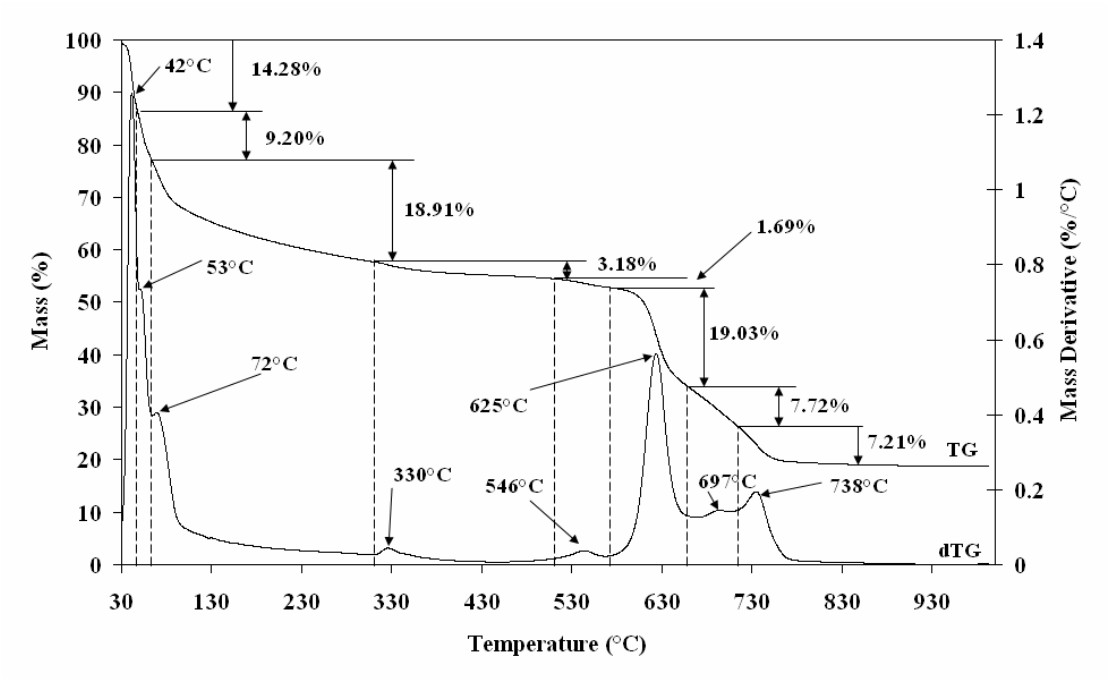
Mass (%)
Mass Derivative (%/°C)
Temperature (°C)
42°C
14.28%
9.20%
18.91%
53°C
72°C
3.18%
1.69%
19.03%
625°C
7.72%
7.21%
TG
330°C
546°C
697°C
738°C
dTG

Figure 7